Physica E: Low-dimensional Systems and Nanostructures 115 (2020) 113645

Contents lists available at ScienceDirect

Physica E: Low-dimensional Systems and Nanostructures

journal homepage: www.elsevier.com/locate/physe

Graphene membrane-based NEMS for study of interface interaction

Andrei I. Siahlo[a], Andrey M. Popov[b], Nikolai A. Poklonski[a,*], Yurii E. Lozovik[b,c], Sergey A. Vyrko[a]

[a] Physics Department, Belarusian State University, Nezavisimosti Ave. 4, Minsk, 220030, Belarus
[b] Institute for Spectroscopy Russian Academy of Science, Fizicheskaya Str. 5, Troitsk Moscow, 108840, Russia
[c] Moscow Institute of Electronics and Mathematics, National Research University Higher School of Economics, Moscow, 101000, Russia

ARTICLE INFO

Keywords:
Graphene membrane
Interatomic potential
Interface interaction
Van der Waals interaction
NEMS

ABSTRACT

The scheme and operational principles of graphene-based nanoelectromechanical system (NEMS) for study of interaction between graphene and surface of a sample is proposed. In such a NEMS multilayer graphene membrane bends due to van der Waals attraction between surface of graphene membrane and surface of a sample attached to a manipulator. An analysis of the NEMS total energy balance shows that the NEMS is bistable and abrupt transition between the stable states occurs if the sample is moved toward and backward the membrane. The detection of the interface distances corresponding to these transitions can be used to fit parameters of interatomic potentials for interaction between atoms of the surfaces of the graphene membrane and the sample. The analytical expression for dependences of this transition distances on NEMS sizes and parameters of the potential are derived on example of Lennard-Jones potential. For graphene-graphene interaction the transition distance is estimated to be from several nanometers to several tens nanometers for possible sizes of the proposed NEMS and thus can be measurable for example by transmission electron microscopy. Possibility of this NEMS implementation and application to study graphene-metal interaction are discussed.

1. Introduction

A set of physical phenomena in bilayer and few layer graphene systems originate from relative rotation or displacement of the layers. Band gap and quantum transport depend on stacking of layers in trilayer graphene [1] and relative orientation of layers in bilayer graphene [2,3]. Superconductivity in twisted graphene bilayers have been recently reported [4]. Dynamic phenomena based on relative rotation or displacement of graphene layers include atomic-scale slip-stick motion of a graphene flake attached to a STM tip [5,6], rotation-assisted diffusion of a graphene flake [7], self-retracting motion of the layers at their telescopic extension [8,9] and motion of stacking dislocation by electric field [10].

In spite of the importance of interaction between graphene layers for fundamental physics and applications, only few works have been devoted even to determination of graphene-graphene binding energy. Namely, the following values of the binding energy have been obtained: -43 ± 5 meV/atom based on heat of wetting data [11], -52 ± 5 meV/atom using thermal desorption spectroscopy of polyaromatic hydrocarbons from graphite surface [12], -35^{+15}_{-10} meV/atom [13], and -31 ± 2 meV/atom [14] based on models which describe the balance between elastic and interlayer interaction energies to reproduce the geometry of cross-section of collapsed multiwalled carbon nanotubes and multilayer graphene flake above a step of a graphite surface, respectively. Thus the considerable scatter of the obtained values of the graphene-graphene binding energy have been revealed by experimental studies using different techniques. The comprehensive first-principle calculations which give -56 ± 6 meV/atom by quantum Monte Carlo method [15] and -36 [16] and -48 meV/atom [17] using random phase approximation (RPA) should be also mentioned whereas numerous methods based on density functional theory with corrections for van der Waals interactions give the values from -47 to -83 meV/atom [18]. As for graphene-metal interaction so far as we know no experimental values on forces and energies of interface interaction between graphene and metals whereas calculations of graphene-metal interface energetics using RPA are available [19,20]. Thus elaboration of new techniques which intend to measure physical quantities related with energetics of interface interaction is very actual task.

Particularly the importance of accurate measurements of energetic characteristics of graphene-graphene and graphene-metal interface interaction is related with use of such characteristics as reference data for fitting of parameters of classical interatomic potentials. We consider this problem on example of 6–12 Lennard-Jones (LJ) potential [21] which is well-accepted for description of interaction energy W_{LJ} between atoms of nonpolar molecules and has the form

* Corresponding author.
E-mail addresses: siahloa@bsu.by (A.I. Siahlo), popov-isan@mail.ru (A.M. Popov), poklonski@bsu.by (N.A. Poklonski), lozovik@isan.troitsk.ru (Y.E. Lozovik).

https://doi.org/10.1016/j.physe.2019.113645
Received 13 April 2019; Received in revised form 5 July 2019; Accepted 17 July 2019
Available online 22 July 2019
1386-9477/

$$W_{LJ} = 4\varepsilon\left(\left(\frac{\sigma}{r}\right)^{12} - \left(\frac{\sigma}{r}\right)^{6}\right) = \frac{B}{r^{12}} - \frac{A}{r^{6}}, \quad (1)$$

where r is the interatomic distance, 'ε and σ' and 'A and B' are the pairs of parameters for the two forms of the LJ potential, respectively. The second term of the LJ potential corresponds to long range van der Waals attraction.

In the case of graphene-graphene interaction the parameters of the LJ potential were fitted to reproduce the interlayer binding energy and equilibrium interlayer spacing for graphite with the c-axis compressibility for graphite reproduced well using these parameters [11,22]. In this case the accuracy of the parameter fitting is determined by the scatter of the experimental data for the interlayer binding energy.

Analogously the values of the binding energy and the equilibrium spacing between graphene and metal surface obtained using RPA-based calculations have been applied to obtain the parameters of interatomic LJ potential for graphene-nickel interaction [23]. However for some of metals such as nickel or cobalt two minima (which correspond to covalent and van der Waals binding) in the dependence of the interaction energy on the spacing between the graphene and metal surface have been found using RPA-based calculations [20]. For some other metals (such as Au) these calculations give one minimum in these dependence but the shape of the dependence considerably differs from the shape which correspond to LJ potential for interaction between atoms of the surfaces [20]. That is using of LJ potential can be inadequate for description of graphene-metal interaction. Note that the attraction term of the LJ potential can be in principle adequate at nanometer scale for graphene-metal interaction even in a case where the overall LJ potential is inadequate at distances which are close to the equilibrium spacing between graphene and metal surfaces.

Thus at present time the parameters of classical interatomic potentials for description of interaction between graphene and other surfaces have been fitted to reproduce the reference data which corresponds to equilibrium spacing between the surfaces, with considerable scatter of experimental data for graphene-graphene interaction and only theoretical data are available for graphene-metal interface interaction. However in many cases adequate description of interaction between graphene layers or between graphene layer and other surface at nanometer scale is necessary (that is at distances which are several times greater than equilibrium interface distances). For instance, the Lennard-Jones potential have been applied to describe the interaction between graphene layers in simulation of a carbon nanoscroll formation from a graphene layer [24] and in calculation of operational characteristics of graphene-based memory cells [25–28]. The Lennard-Jones potential describing carbon-metal interaction has been also used in consideration of memory cells based on carbon nanotubes [29,30]. Thus the direct measurements of characteristics of interaction between graphene layers and between graphene and other surfaces at nanometer scale is an actual task for fitting of parameters of interatomic potentials.

The implementation of resonators based on graphene membrane as pressure [31,32] and mass [33] sensors and microphones [34] demonstrates availability of graphene membrane-based NEMS. Graphene membrane based memory cell have been also considered [26]. Here we propose a scheme and operational principles of the graphene membrane-based NEMS for measurement of characteristics of interface interaction between graphene and other surfaces at nanometer scale. This gives the unicum possibility to study pure van der Waals interaction between surfaces and to get new reference data for fitting of parameters of interatomic potentials describing interaction between atoms of neighbor graphene layers and between atoms of graphene layer and atoms of other materials.

wThe paper is organized in the following way. Concept and operational principles of the proposed NEMS are presented in Section 2. Section 3 is devoted to calculations of operation characteristics of the NEMS on example of graphene-graphene interaction. Conclusions are summarized and possibility of the NEMS implementation is discussed in Section 4.

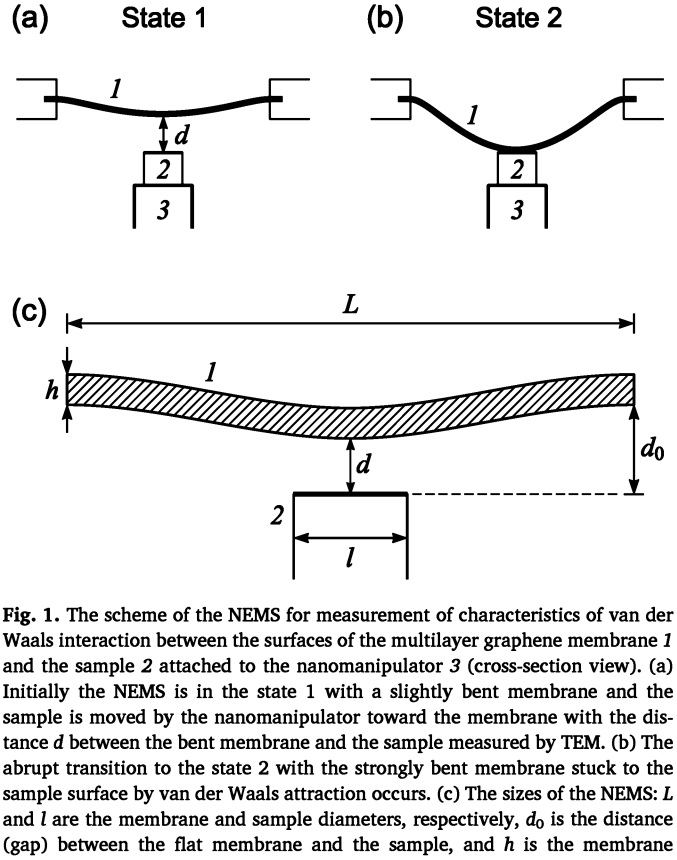

Fig. 1. The scheme of the NEMS for measurement of characteristics of van der Waals interaction between the surfaces of the multilayer graphene membrane *1* and the sample *2* attached to the nanomanipulator *3* (cross-section view). (a) Initially the NEMS is in the state 1 with a slightly bent membrane and the sample is moved by the nanomanipulator toward the membrane with the distance d between the bent membrane and the sample measured by TEM. (b) The abrupt transition to the state 2 with the strongly bent membrane stuck to the sample surface by van der Waals attraction occurs. (c) The sizes of the NEMS: L and l are the membrane and sample diameters, respectively, d_0 is the distance (gap) between the flat membrane and the sample, and h is the membrane thickness.

2. Concept of NEMS

The scheme of the proposed NEMS for study of interaction between graphene and surfaces of any materials is shown in Fig. 1a and b. This NEMS consists of a multilayer graphene membrane (*1*) placed over a sample (*2*) with a flat surface attached to a nanomanipulator (*3*). Thus the sample can be moved by the nanomanipulator toward and backward the membrane. The surface of the sample can be covered by graphene or graphite in a case where graphene-graphene interaction is studied or can be atomically precise surface of any other material in a case where interface interaction between graphene and this material is studied. The operational principles of this NEMS are based on the so-called bistability of the system, i.e. the presence of the two minima in the potential energy of the system as a function of the relative position of movable parts. Namely, the system has two stable states: state 1 with the slightly bent membrane without contact between the surface of the sample and the membrane (Fig. 1a) and state 2 with the strongly bent membrane stuck to the surface of the sample by the van der Waals force so that the distance between the surfaces of the membrane and the sample is close to the equilibrium distance (Fig. 1b). The transitions between states 1 and 2 and between states 2 and 1 take place when the sample is moved by the nanomanipulator toward and backward the membrane, respectively. Below we show that these transitions occur with abrupt change of the distance between the surface of the sample and the surface of the graphene membrane. Moveover we show that the sticking distance where the abrupt transition from state 1 to state 2 occurs at the sample motion towards the membrane is determined mainly by the balance between the elastic force of bent membrane and van der Waals attraction between the surfaces of the graphene membrane and the sample whereas contribution of the repulsion between these surfaces into this balance is negligible. Thus a measurement of this distance can be used to determine characteristics of van der Waals attraction between the surfaces. For example such a measurement can

be performed by transmission electron microscope (TEM). The schemes of experiment where manipulations with nanometer-size objects using a nanomanipulator are controlled by TEM imaging are available about 20 years [35].

3. Calculated characteristics of NEMS

For a simple model, we consider the NEMS based on a circular multilayer graphene membrane which has a clamped edge and a sample with a circular flat surface covered by graphene or graphite. The operational characteristics of the NEMS are determined by the following fixed sizes: the membrane diameter L, the sample diameter l, and the membrane thickness h (see Fig. 1c). Along with these fixed sizes there are two sizes which are changing during the NEMS operation: the distance d_0 between surface of the sample and center of the flat membrane (which is tuned by the nanomanipulator) and the distance d between surface of the sample and the bent membrane. Note that both distances d_0 and d can be measured in principle. The sticking distances d_{0s} and d_s and the detachment distances d_{0d} and d_d correspond to the abrupt transitions between states 1 and 2 and between states 2 and 1, respectively.

Let us obtain the expressions which relate fixed sizes of the NEMS, L, l, and h, the sticking distances d_{0s} and d_s or the detachment distances d_{0d} and d_d and parameters of classical potential describing interaction between atoms of the membrane and the sample surfaces. For this purpose we consider energy balance of the NEMS on the example of the LJ potential (1). The total energy W of the NEMS is the sum of the van der Waals interaction energy W_{vdW} between the membrane and the sample and the elastic energy W_{el} of the membrane, $W = W_{vdW} + W_{el}$.

The elastic energy W_{el} of the circular membrane with a clamped edge which is loaded in the center has the form [36]:

$$W_{el} = 16\pi D\left(\frac{2}{L}\right)^2\frac{(d_0-d)^2}{2}, \tag{2}$$

where $d_0 - d$ is the deflection of the membrane center and D is the membrane flexural rigidity

$$D = \frac{E\,h^3}{12(1-\nu^2)}, \tag{3}$$

where E and ν are the Young's modulus and the Poisson's ratio, respectively, h is the membrane thickness. According to the measurements of the flexural rigidity of the multilayer graphene membranes, formula (3) is applicable for membranes with thickness h exceeding 3 nm [37] (about 10 graphene layers) with the values of elastic constants $E = 0.92$ TPa, $\nu = 0.16$ measured for graphite [38]. Here we use these values of the Young's modulus and the Poisson's ratio.

Here we consider the case where $d \ll l$ and $l \ll L$. In this case the van der Waals interaction energy W_{vdW} between the parallel membrane and the sample located at the distance d from the membrane center is given by Ref. [26]:

$$W_{vdW} = \frac{\pi^2 l^2 \varepsilon}{S_a^2}\left(\frac{\sigma^{12}}{5d^{10}} - \frac{\sigma^6}{2d^4}\right), \tag{4}$$

where S_a is the area per one atom of graphene layer, $S_a = 2.619$ Å^2. The parameters of the LJ potential $\varepsilon = 2.757$ meV and $\sigma = 3.393$ Å $= 0.3393$ nm fitted [22] to reproduce the interlayer binding energy, equilibrium interlayer spacing and c-axis compressi-bility of graphite are used at calculations below.

Thus the total energy of the NEMS takes the form

$$W = W_{vdW} + W_{el} = \frac{\pi^2 l^2 \varepsilon}{S_a^2}\left(\frac{\sigma^{12}}{5d^{10}} - \frac{\sigma^6}{2d^4}\right) + \\ + \frac{32\pi D(d_0-d)^2}{L^2} = \frac{a}{5d^{10}} - \frac{b}{2d^4} + c(d_0-d)^2, \tag{5}$$

where

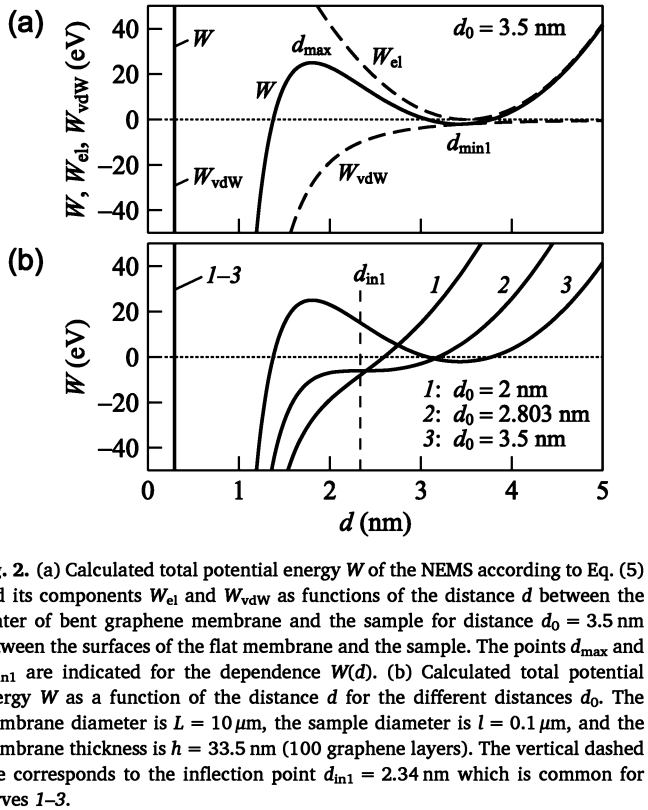

Fig. 2. (a) Calculated total potential energy W of the NEMS according to Eq. (5) and its components W_{el} and W_{vdW} as functions of the distance d between the center of bent graphene membrane and the sample for distance $d_0 = 3.5$ nm between the surfaces of the flat membrane and the sample. The points d_{max} and d_{min1} are indicated for the dependence $W(d)$. (b) Calculated total potential energy W as a function of the distance d for the different distances d_0. The membrane diameter is $L = 10\,\mu$m, the sample diameter is $l = 0.1\,\mu$m, and the membrane thickness is $h = 33.5$ nm (100 graphene layers). The vertical dashed line corresponds to the inflection point $d_{in1} = 2.34$ nm which is common for curves *1–3*.

$$a = \frac{\pi^2 l^2 \varepsilon}{S_a^2}\sigma^{12}, \quad b = \frac{\pi^2 l^2 \varepsilon}{S_a^2}\sigma^6, \quad c = \frac{32\pi D}{L^2}. \tag{6}$$

The dependences of both components of the total energy W of the NEMS, the elastic energy $W_{el}(d)$ and the van der Waals interaction energy $W_{vdW}(d)$, on the distance d between the surfaces of the bent membrane and the sample at the fixed distance d_0 between the surfaces of the flat membrane and the sample are shown in Fig. 2a. The bistability of the NEMS has its origin in presence of the single minimum in dependences of both energies $W_{el}(d)$ and $W_{vdW}(d)$ at different distances d. To show loss of the bistability of the NEMS with the change of the fixed distance d_0 between the surfaces of the flat membrane and the sample the dependences $W(d)$ of the total energy W of the NEMS on the distance d between the surfaces of the bent membrane and the sample are shown in Fig. 2b for three fixed distances d_0. Namely, line *3* corresponds to some distance d_{0b} where the system is bistable (that is two minima in the dependence $W(d)$ are present) and line *2* corresponds to sticking distance $d_{0s} < d_{0b}$ where the second minimum in the dependence $W(d)$ is vanished and the abrupt transition from state 1 to state 2 occurs. This means that sticking of the membrane takes place when the sample is moved toward the membrane by the nanomanipulator. Analogously the abrupt transition from state 2 to state 1 (detachment of the membrane) occurs at backward motion of the sample. (Line *1* corresponds to distance $d_0 < d_{0s}$ where the dependence $W(d)$ also has only the first minimum.) The loss of the bistability of the NEMS, that is the sticking and detachment of the membrane at forward and backward motion of the sample, respectively, means hysteresis in the dependences of the total potential energy $W(d_0)$ and the distance $d(d_0)$ between the surfaces of the bent membrane and the sample on the distance d_0 between the surfaces of the flat membrane and the sample (see Fig. 3).

For the bistable NEMS the function $W(d)$ has two minima at d_{min1} and d_{min2} which correspond to the stable states 1 and 2, respectively, the maximum d_{max} between these minima and two inflection points at d_{in1} and d_{in2} between d_{min1} and d_{max} and between d_{max} and d_{min2}, respectively. For the sticking distance d_{0s} between the surface of the

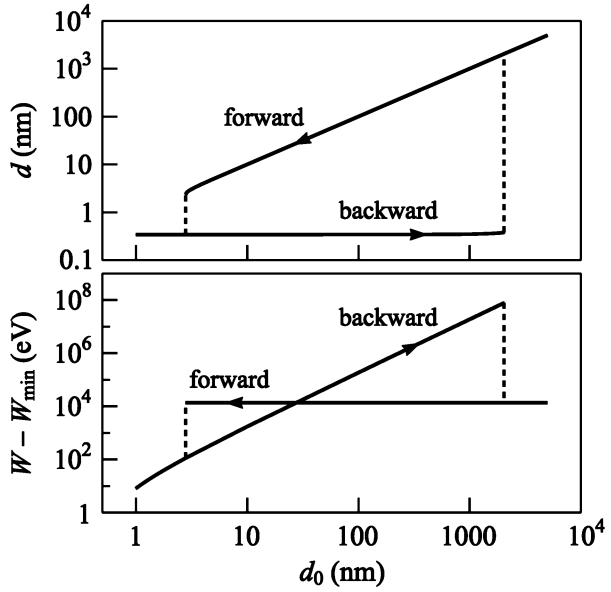

Fig. 3. Calculated dependences of the distance d between the surfaces of the bent membrane and the sample (top panel) and the total potential energy W of the NEMS (bottom panel) on the distance d_0 between the surfaces of the flat membrane and the sample at forward and backward motion of the sample (shown by arrows). In order to show the energy W in a double logarithmic scale the minimum value W_{min} of the energy W (at the distance $d_0 = 0.34$ nm) is used as a reference.

sample and center of the flat membrane (where the transition from state 1 to state 2 takes place) the values of d_{max}, d_{in1}, and d_{min1} coincide (see Fig. 2). Similarly, for the detachment distance d_{0d} the values of d_{max}, d_{in2}, and d_{min2} coincide.

The inflection points are determined by the condition $\partial^2 W/\partial d^2 = 0$ which using Eq. (5) takes the form

$$\frac{11a}{d^{12}} - \frac{5b}{d^6} + c = 0. \tag{7}$$

The Eq. (7) does not contain distance d_0 between the surface of the sample and the center of the flat membrane. Therefore the values of the inflection points d_{in1} and d_{in2} do not change at moving of the sample by the nanomanipulator. Thus the inflection points determined by Eq. (7) are the sticking distances d_s and the detachment distances d_d between the surface of the sample and the bent membrane

$$d_{in1} = d_s = \left(\frac{5b+\sqrt{25b^2-44ac}}{2c}\right)^{1/6},$$
$$d_{in2} = d_d = \left(\frac{5b-\sqrt{25b^2-44ac}}{2c}\right)^{1/6}. \tag{8}$$

As discussed above the distances d_s and d_d are also roots of the equation $\partial W/\partial d = 0$ which takes the form

$$c(d - d_0) + \frac{b}{d^5} - \frac{a}{d^{11}} = 0. \tag{9}$$

where a, b, and c are defined by Eq. (6).

The sticking distance d_{0s} and the detachment distance d_{0d} between surface of the sample and center of the flat membrane are found by substituting d_s and d_d, respectively (which are determined by Eq. (8)), into Eq. (9). Thus, it yields

$$d_{0s} = d_s + \frac{b}{cd_s^5} - \frac{a}{cd_s^{11}}, \quad d_{0d} = d_d + \frac{b}{cd_d^5} - \frac{a}{cd_d^{11}}. \tag{10}$$

The concept of the NEMS proposed in Section 2 is based on measurements of the sticking distance d_s between the surface of the sample and the bent membrane while moving sample toward the membrane

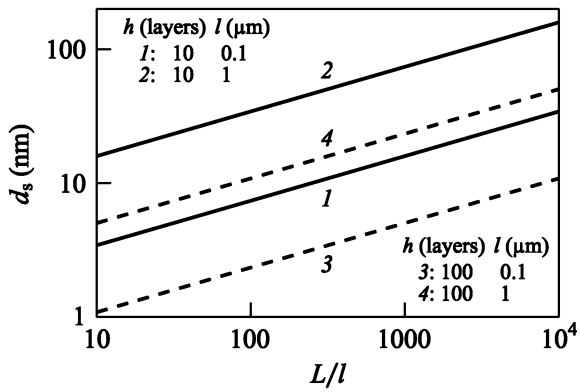

Fig. 4. Calculated dependences of the sticking distance d_s (in nm) according to Eq. (11) on the ratio of the membrane and sample diameters L/l for NEMS with the different membrane thicknesses $h = 33.5$ nm (100 graphene layers; dashed lines) and $h = 3.35$ nm (10 graphene layers; solid lines) and different sample diameters $l = 0.1$ μm (lines *1* and *3*) and $l = 1$ μm (lines *2* and *4*).

(positioning the sample at the distance d_{0s} from the flat membrane). Let us obtain the dependence of the measurable sticking distances d_s and d_{0s} on the fixed sizes of the NEMS. As shown below, the repulsive term can be disregarded at the distance d_s in the van der Waals interaction energy W_{vdW} which is determined by Eq. (4) for all considered fixed sizes of the NEMS. [Thus only the attractive term $-A/r^6 = -4\varepsilon\sigma^6/r^6$ with the single parameter A can be taken into account in the LJ potential (1).] In this case the sticking distance d_s from Eq. (8) (formally at $a \to 0$) takes the form

$$d_s = \frac{1}{2}\left(\frac{5\pi A}{2D}\right)^{1/6}\left(\frac{lL}{S_a}\right)^{1/3}, \tag{11}$$

while the sticking distance d_{0s} from Eq. (10) takes the form

$$d_{0s} = \frac{6}{5}d_s = \frac{3}{5}\left(\frac{5\pi A}{2D}\right)^{1/6}\left(\frac{lL}{S_a}\right)^{1/3}. \tag{12}$$

Let us use Eq. (11) to consider the range of the distances d_s for the NEMS with the different membrane thicknesses and membrane and sample diameters (see Fig. 4). The calculated sticking distance d_s ranges from 3 to 100 nm and from 1 to 30 nm for the NEMS based on 10-layer and 100-layer graphene membranes, respectively. Note that even for the smallest sticking distance $d_s = 0.5$ nm for considered sizes of the NEMS (which is obtained for sample diameter $l = 2$ nm and 10-layer membrane diameter $L = 200$ nm) the relative difference between values of d_s calculated using Eqs. (10) and (11) is only 0.03. This relative difference decreases with the increase of the sticking distance. The distances near the upper limits of the calculated distances ranges which can be easily measurable by TEM correspond to the sample diameter $l = 1$ μm and membrane diameter $L = 10$ mm. Such sizes of the sample and membrane can be easily realized by modern technology. For example, microphone implemented recently is based on 60-layer graphene membrane with the diameter of 5–12 mm [34]. Note that we consider in Fig. 4 the sizes of NEMS which is designed to measure the sticking distances d_s. For the considered sizes of NEMS the detachment of the membrane without considerable deformation of the membrane is possible only for the NEMSs with sufficiently large values of the membrane thickness h and the ratio L/l of the membrane L and sample l diameters.

4. Discussion and conclusions

We propose the NEMS designed to study interaction between graphene and surface of a sample. This NEMS is based on a multilayer graphene membrane which bends due to van der Waals attraction to surface of a sample. The performed analysis of the balance between

elastic energy of the graphene membrane and energy of interaction between surfaces of the membrane and sample shows that the NEMS is bistable and abrupt transitions between the stable states, namely, sticking of the membrane to the sample and detachment of the membrane, occurs if the sample is moved toward and backward the membrane, respectively. We propose to measure the sticking and detachment distances between the surfaces of the membrane and sample corresponding to these transitions. The analytical expression for these distances in terms of the sizes of the NEMS parts, the elastic constants of the graphene membrane and the parameters of the Lennard-Jones (LJ) potential for interaction between atoms of the surfaces are derived.

The operation of the proposed NEMS is considered on example of graphene-graphene interaction. The membrane sticking distance is estimated to be from 1 nm to about hundred nanometers for possible sizes of the NEMS. Such range of the distances ensures reasonable accuracy for their measurements by TEM.

All previous studies of the interaction between graphene layers [11–14] deal with the interlayer interaction energy at the equilibrium distance between layers where the balance between van der Waals attraction and repulsion between layers takes place. For the estimated range of the membrane sticking distance only attractive term $-A/r^6$ of the LJ potential contributes to the energy balance of NEMS whereas contribution of the repulsive term is negligible. Thus the measurement of the transition distance is also a direct measurement of the parameter A. Such measurements can also be used in combination with other experimental data to determine parameters of the LJ potential or any other interatomic potential which describe interaction between atoms of graphene and a sample.

Let us discuss the application of the proposed NEMS to study graphene-metal interaction. The binding energy for a graphene layer on metal surface have been obtained on the basis of the adiabatic-connection fluctuation–dissipation theorem in the random phase approximation for a wide set of metals (Ni, Co, Cu, Pd, Pt, Au, Ag, and Al) [20]. For all considered metals the calculated values of the binding energy range from -90 to -52 meV per carbon atom. This value is about the value for the binding energy between graphene layers or only twice greater. Thus the consideration of the NEMS operation performed for the case of graphene-graphene interaction shows the possibility of the NEMS application to study of graphene-metal interaction.

A wide set of graphene transfer methods have been elaborated (see Ref. [39] for a review). As a result of this progress in nanotechnology various graphene membrane-based NEMS, including microphones [34] and pressure [31,32] and mass [33] sensors, have been implemented. Operation with a sample by a nanomanipulator and simultaneous imaging of this process by TEM become possible about 20 years ago [35]. And lastly implementation of pristine interfaces between 2D materials and other materials should be mentioned (see Ref. [40] for a recent review). All these gives us a cause for the optimism that the proposed NEMS can be realized using methods of modern nanotechnology.

Data availability

The raw data required to reproduce these findings are available to download [41].

Acknowledgments

A.I.S., N.A.P., and S.A.V. acknowledge support by the Belarusian Republican Foundation for Fundamental Research (Grant No. F18R-253) and Belarusian National Research Program "Convergence-2020". A.M.P. and Y.E.L. acknowledge support by the Russian Foundation for Basic Research (Grant No. 18-52-00002).

References

[1] W. Bao, L. Jing, J. Velasco, Y. Lee, G. Liu, D. Tran, B. Standley, M. Aykol, S.B. Cronin, D. Smirnov, Stacking-dependent band gap and quantum transport in trilayer graphene, Nat. Phys. 7 (2011) 948–952, https://doi.org/10.1038/NPHYS2103.

[2] R. Bistritzer, A.H. MacDonald, Transport between twisted graphene layers, Phys. Rev. B 81 (2010) 245412, https://doi.org/10.1103/PhysRevB.81.245412.

[3] R. Bistritzer, A.H. MacDonald, Moiré bands in twisted double-layer graphene, Proc. Natl. Acad. Sci. 108 (2011) 12233–12237, https://doi.org/10.1073/pnas.1108174108.

[4] Y. Cao, V. Fatemi, S. Fang, K. Watanabe, E.K.T. Taniguchi, P. Jarillo-Herrero, Unconventional superconductivity in magic-angle graphene superlattices, Nature 556 (2018) 43–50, https://doi.org/10.1038/nature26160.

[5] M. Dienwiebel, G.S. Verhoeven, N. Pradeep, J.W.M. Frenken, J.A. Heimberg, H.W. Zandbergen, Superlubricity of graphite, Phys. Rev. Lett. 92 (2004) 126101, https://doi.org/10.1103/PhysRevLett.92.126101.

[6] A.E. Filippov, M. Dienwiebel, J.W.M. Frenken, J. Klafter, M. Urbakh, Torque and twist against superlubricity, Phys. Rev. Lett. 100 (2008) 046102, https://doi.org/10.1103/PhysRevLett.100.046102.

[7] I.V. Lebedeva, A.A. Knizhnik, A.M. Popov, O.V. Ershova, Y.E. Lozovik, B.V. Potapkin, Fast diffusion of a graphene flake on a graphene layer, Phys. Rev. B 82 (2010) 155460, https://doi.org/10.1103/PhysRevB.82.155460.

[8] Q. Zheng, B. Jiang, S. Liu, Y. Weng, L. Lu, Q. Xue, J. Zhu, Q. Jiang, S. Wang, L. Peng, Self-retracting motion of graphite microflakes, Phys. Rev. Lett. 100 (2008) 067205, https://doi.org/10.1103/PhysRevLett.100.067205.

[9] A.M. Popov, I.V. Lebedeva, A.A. Knizhnik, Y.E. Lozovik, B.V. Potapkin, Molecular dynamics simulation of the self-retracting motion of a graphene flake, Phys. Rev. B 84 (2011) 245437, https://doi.org/10.1103/PhysRevB.84.245437.

[10] M. Yankowitz, J.I.-J. Wang, A.G. Birdwell, Y.-A. Chen, K. Watanabe, T. Taniguchi, P. Jacquod, P. San-Jose, P. Jarillo-Herrero, B.J. LeRoy, Electric field control of soliton motion and stacking in trilayer graphene, Nat. Mater. 13 (2014) 786–789, https://doi.org/10.1038/nmat3965.

[11] L.A. Girifalco, R.A. Lad, Energy of cohesion, compressibility, and the potential energy functions of the graphite system, J. Chem. Phys. 25 (1956) 693–696, https://doi.org/10.1063/1.1743030.

[12] R. Zacharia, H. Ulbricht, T. Hertel, Interlayer cohesive energy of graphite from thermal desorption of polyaromatic hydrocarbons, Phys. Rev. B 69 (2004) 155406, https://doi.org/10.1103/PhysRevB.69.155406.

[13] L.X. Benedict, N.G. Chopra, M.L. Cohen, A. Zettl, S.G. Louie, V.H. Crespi, Microscopic determination of the interlayer binding energy in graphite, Chem. Phys. Lett. 286 (1998) 490–496, https://doi.org/10.1016/S0009-2614(97)01466-8.

[14] Z. Liu, J.Z. Liu, Y. Cheng, Z. Li, L. Wang, Q. Zheng, Interlayer binding energy of graphite: a mesoscopic determination from deformation, Phys. Rev. B 85 (2012) 205418, https://doi.org/10.1103/PhysRevB.85.205418.

[15] L. Spanu, S. Sorella, G. Galli, Nature and strength of interlayer binding in graphite, Phys. Rev. Lett. 103 (2009) 196401, https://doi.org/10.1103/PhysRevLett.103.196401.

[16] E. Mostaani, N.D. Drummond, V.I. Fal'ko, Quantum Monte Carlo calculation of the binding energy of bilayer graphene, Phys. Rev. Lett. 115 (2015) 115501, https://doi.org/10.1103/PhysRevLett.115.115501.

[17] S. Lebègue, J. Harl, T. Gould, J.G. Ángyán, G. Kresse, J.F. Dobson, Cohesive properties and asymptotics of the dispersion interaction in graphite by the random phase approximation, Phys. Rev. Lett. 105 (2010) 196401, https://doi.org/10.1103/PhysRevLett.105.196401.

[18] I.V. Lebedeva, A.V. Lebedev, A.M. Popov, A.A. Knizhnik, Comparison of performance of van der Waals-corrected exchange-correlation functionals for interlayer interaction in graphene and hexagonal boron nitride, Comput. Mater. Sci. 128 (2017) 48–57, https://doi.org/10.1016/j.commatsci.2016.11.011.

[19] F. Mittendorfer, A. Garhofer, J. Redinger, J. Klimeš, J. Harl, G. Kresse, Graphene on Ni(111): strong interaction and weak adsorption, Phys. Rev. B 84 (2011) 201401, https://doi.org/10.1103/PhysRevB.84.201401.

[20] T. Olsen, K.S. Thygesen, Random phase approximation applied to solids, molecules, and graphene-metal interfaces: from van der Waals to covalent bonding, Phys. Rev. B 87 (2013) 075111, https://doi.org/10.1103/PhysRevB.87.075111.

[21] J.E. Lennard-Jones, Cohesion, Proc. Phys. Soc. 43 (1931) 461–482, https://doi.org/10.1088/0959-5309/43/5/301.

[22] I.V. Lebedeva, A.A. Knizhnik, A.M. Popov, Yu E. Lozovik, B.V. Potapkin, Interlayer interaction and relative vibrations of bilayer graphene, Phys. Chem. Chem. Phys. 13 (2011) 5687–5695, https://doi.org/10.1039/C0CP02614J.

[23] A.S. Sinitsa, T.W. Chamberlain, T. Zoberbier, I.V. Lebedeva, A.M. Popov, A.A. Knizhnik, R.L. McSweeney, J. Biskupek, U. Kaiser, A.N. Khlobystov, Formation of nickel clusters wrapped in carbon cages: towards new endohedral metallofullerene synthesis, Nano Lett. 17 (2017) 1082–1089, https://doi.org/10.1021/acs.nanolett.6b04607.

[24] X. Shi, N.M. Pugno, H. Gao, Tunable core size of carbon nanoscrolls, J. Comput. Theor. Nanosci. 7 (2010) 517–521, https://doi.org/10.1166/jctn.2010.1387.

[25] J.W. Kang, K.-S. Kim, O.K. Kwon, Energetic bistability of carbon-nanotube shuttle memory placed on graphene nanoribbon array, J. Comput. Theor. Nanosci. 12 (2015) 387–390, https://doi.org/10.1166/jctn.2015.3740.

[26] A.I. Siahlo, A.M. Popov, N.A. Poklonski, Y.E. Lozovik, S.A. Vyrko, S.V. Ratkevich, Multi-layer graphene membrane based memory cell, Physica E 84 (2016) 348–353, https://doi.org/10.1016/j.physe.2016.08.003.

[27] J.W. Kang, K.W. Lee, Schematics and energetics of bucky shuttle memory on

graphene nanoribbon array, J. Nanosci. Nanotechnol. 16 (2016) 2891–2896, https://doi.org/10.1166/jnn.2016.11068.
[28] E. Lee, J.W. Kang, Molecular dynamics analysis of graphene-based nanoelectromechanical switch, ECS Trans 72 (2016) 1–6, https://doi.org/10.1149/07214.0001ecst.
[29] L. Maslov, Concept of nonvolatile memory based on multiwall carbon nanotubes, Nanotechnology 17 (2006) 2475–2482, https://doi.org/10.1088/0957-4484/17/10/007.
[30] A.M. Popov, E. Bichoutskaia, Y.E. Lozovik, A.S. Kulish, Nanoelectromechanical systems based on multi-walled nanotubes: nanothermometer, nanorelay, and nanoactuator, Phys. Status Solidi A 204 (2007) 1911–1917, https://doi.org/10.1002/pssa.200675322.
[31] A.D. Smith, F. Niklaus, A. Paussa, S. Vaziri, A.C. Fischer, M. Sterner, F. Forsberg, A. Delin, D. Esseni, P. Palestri, M. Östling, M.C. Lemme, Electromechanical piezoresistive sensing in suspended graphene membranes, Nano Lett. 13 (2013) 3237–3242, https://doi.org/10.1021/nl401352k.
[32] J. Aguilera-Servin, T. Miao, M. Bockrath, Nanoscale pressure sensors realized from suspended graphene membrane devices, Appl. Phys. Lett. 106 (2015) 083103, https://doi.org/10.1063/1.4908176.
[33] C. Chen, S. Rosenblatt, K.I. Bolotin, W. Kalb, P. Kim, I. Kymissis, H.L. Stormer, T.F. Heinz, J. Hone, Performance of monolayer graphene nanomechanical resonators with electrical readout, Nat. Nanotechnol. 4 (2009) 861–867, https://doi.org/10.1038/nnano.2009.267.
[34] D. Todorović, A. Matković, M. Milićević, D. Jovanović, R. Gajić, I. Salom, M. Spasenović, Multilayer graphene condenser microphone, 2D Mater. 2 (2015) 045013, https://doi.org/10.1088/2053-1583/2/4/045013.
[35] J. Cumings, A. Zettl, Low-friction nanoscale linear bearing realized from multiwall carbon nanotubes, Science 289 (2000) 602–604, https://doi.org/10.1126/science.289.5479.602.
[36] S. Timoshenko, S. Woinowsky-Krieger, Theory of Plates and Shells, McGraw-Hill, New York, 1959.
[37] M. Poot, H.S.J. van der Zant, Nanomechanical properties of few-layer graphene membranes, Appl. Phys. Lett. 92 (2008) 063111, https://doi.org/10.1063/1.2857472.
[38] O.L. Blakslee, D.G. Proctor, E.J. Seldin, G.B. Spence, T. Weng, Elastic constants of compression-annealed pyrolytic graphite, J. Appl. Phys. 41 (1970) 3373–3382, https://doi.org/10.1063/1.1659428.
[39] J. Kang, D. Shin, S. Bae, B.H. Hong, Graphene transfer: key for applications, Nanoscale 4 (2015) 5527–5537, https://doi.org/10.1039/c2nr31317k.
[40] Y. Liu, Y. Huang, X. Duan, Van der Waals integration before and beyond two-dimensional materials, Nature 567 (2019) 323–333, https://doi.org/10.1038/s41586-019-1013-x.
[41] N.A. Poklonski, A.I. Siahlo, S.A. Vyrko, Y.E. Lozovik, A.M. Popov, Data for: Graphene Membrane-Based NEMS for Study of Interface Interaction, Mendeley Data, 2019, https://doi.org/10.17632/yv7hxccj6x.1.